Chapter 2

Neutrinoless Double Beta Decay (NDBD) and Lepton Flavor Violation (LFV) using A_4 Modular Symmetry in Minimal Inverse Seesaw

In this chapter of the thesis we will discuss two of the important BSM phenomena i.e. neutrinoless double-beta decay (NDBD) and lepton flavor violating processes (LFV). These two processes are a crucial part of this thesis. NDBD is related to the decay processes where lepton number is violated by two units, $\Delta L = \pm 2$. It is clear from various literatures that for a better understanding and explanation of these relevant topics, one has to extend the SM with additional particles. Accordingly we have carried out our work in one of such extensions, known as minimal inverse seesaw, ISS(2,3). Apart from the particles present in the SM, this mechanism is augmented with two right-handed neutrinos and three sterile fermions which are singlet under the SM gauge group $SU(3)_C \otimes SU(2)_L \otimes U(1)_Y$. These additional particles facilitate to obtain tiny neutrino masses and the related phenomenological quantities in the desired 3σ range. Using this mechanism we have constructed a model by applying $\Gamma(3)$ modular group. This finite modular

group $\Gamma(3)$ of level $N = 3$ is isomorphic to the discrete symmetry group A_4. Consequently the group A_4 plays a vital role in developing the model of our work. To study the effect of neutrinoless double beta decay, we have calculated the Majorana effective mass (m_{eff}/m_{ee}) of electron neutrino for this model. As predicted by different NDBD experiments the value of m_{eff} is found to lie around ≤ 0.165 eV. In this work we have also studied the lepton flavor violating process $\mu \to e\gamma$. For this purpose we have calculated the branching ratio and found that it lies within the range allowed by the relevant experiments i.e. $\text{BR}(\mu \to e\gamma) < 5.7 \times 10^{-13}$. Along with these two prominent BSM phenomena, we have also evaluated the neutrino parameters in this work.

2.1 Introduction

Inverse seesaw (ISS) is one of the important frameworks that is used to explore new physics which are out of reach of the Standard Model. This extension of SM contains right-handed neutrinos and sterile fermions. Although in the standard notation there are three families for each of these particles, this number varies according to the need of the setup. For example, in some instances there may be two right-handed neutrinos and two sterile fermions in the framework. In some other cases there may be more number of right-handed neutrinos than sterile fermions and vice-versa. One such version of this mechanism is called minimal inverse seesaw, ISS(2,3). As stated earlier, it contains two right-handed neutrinos and three sterile fermions. In this thesis most of the work is done in this variant of inverse seesaw. One of the prime advantages of ISS over the other mechanisms is its ability to bring down the mass of right-handed neutrinos to TeV scale. This is possible because of the presence of sterile fermions in the mechanism. A detailed study on inverse seesaw and its different variants can be found in the literatures [134, 135, 136, 8, 137].

The quantum phenomenon of neutrino oscillation established two important properties of neutrinos. This process showed that there must be mixing among the neutrinos as they propagate through space. It also highlighted the need for existence of tiny mass of neutrino for successful oscillation of one flavor to another.

For the active neutrinos there are three mixing angles and two mass-squared differences in the standard scenario. These angles associated with neutrinos are named as solar mixing angle (θ_{12}), atmospheric mixing angle (θ_{23}) and reactor mixing angle (θ_{13}) [49, 138]. It is interesting to note that the solar and atmospheric mixing angles are reasonably large, whereas the reactor mixing angle is relatively small. In fact the angle θ_{13} was found to have a non-zero value recently in the year 2012. Prior to this it was considered to be zero. On the other hand, only two mass-squared differences are measured at the experiments. This leads to two types of mass orderings of neutrinos, normal and inverted ordering/hierarchy [139, 140]. Though the absolute mass of individual neutrinos are not known, cosmological observations suggest that the sum of absolute mass of the neutrinos should be $\sum m_\nu \leq 0.12$ eV.

In this chapter we emphasize a detailed study of lepton number violating process in minimal inverse seesaw. This LNV process holds the answer to the question about nature of neutrinos: whether they are Dirac or Majorana particles. One of the parameters that characterises this process is the effective Majorana mass of electron neutrino. As per KamLAND-ZEN and other experiments which are searching for NDBD, the latest bound on effective mass is found to be < 0.165 eV. In ISS(2,3) the mixing that takes place between light and heavy neutrinos alters the usual expression of effective mass. We have discussed this modification in later sections of the chapter. Along with NDBD we have also studied the processes where violation of flavor of the charged leptons are observed. These cLFV processes remain highly suppressed in Standard Model. But some of the current experiments like MEG collaboration, SINDRUM II etc. hint at the presence of such flavor violating decays. In our work we have analysed the common two-body cLFV decay channel $\mu \to e\gamma$. The important quantity that describes this type of decays is their branching ratio. Accordingly in this work we have calculated the branching ratio for the decay of our interest. Likewise for NDBD we have evaluated the effective mass of electron neutrino. We have assessed these two interesting processes for the model of our work.

This chapter contains one of the models that we have constructed in the framework of minimal inverse seesaw. In order to determine the interactions among

different fields of the model we have used the popular A_4 modular symmetry. One of the prime motivation of using modular symmetry is to tackle the problem of many flavons that are needed in case of discrete flavor symmetry [141, 142]. With modular symmetry the number of flavons required in a work is significantly reduced. Accordingly, in our models we needed only a single flavon to construct the desired Lagrangian. Moreover the Yukawa couplings are expressed as functions of the complex modulus τ. A brief introduction of modular symmetry is given in the first chapter of the thesis.

This chapter is arranged as follows: section (2.2) contains about the setup of our work. Here we have discussed in great detail about the development of the model of our work. In sections (2.3) and (2.4) we have discussed about the neutrinoless double beta decay and non-unitarity condition of the mixing matrix. A brief summary about LFV processes is present in section (2.5). All the findings and discussions about the results are presented in section (2.6). Lastly in section (2.7) we present a brief summary of the entire work.

2.2 Description of the Model

This section of the chapter contains the first model that we have constructed in our thesis. The mechanism of minimal inverse seesaw serves as the basis for building this model. As we know, the ISS(2,3) contains a pair of $SU(2)\otimes U(1)$ singlet right-handed neutrinos, $N_i(i = 1, 2)$ and three neutral gauge singlet fermions, $S_i(i = 1, 2, 3)$. In our work discrete modular symmetry plays a very crucial role in developing the Lagrangian of the model. In particular we have extensively used A_4 modular symmetry in our work. Apart from A_4 modular group, we have also used Z_3 symmetry in this work. In the next paragraph we will discuss about the particles present in this model and the charges assigned to them under different groups which are used to obtain the desired interaction terms of this formalism.

As evident in various articles [143, 144, 145], the level $N = 3$ modular group $\Gamma(3)$ is isomorphic to the discrete symmetry group A_4. This non-abelian group plays a very crucial role in model building. It has four irreducible representations,

three of which are singlets and one of them denotes triplet representation. The notation for the singlets are $1, 1', 1''$. The triplet is further divided into symmetric and anti-symmetric components, 3_S and 3_A. As per convenience, we assign these representations to the different particles present in the model. Accordingly, the lepton doublets (L) transform as A_4 triplets and right handed charged leptons $E_i(i = e, \mu, \tau)$ transforms as $1, 1''$ and $1'$, respectively. The two right-handed neutrinos N_1 and N_2 are considered as $1'$ and $1''$, whereas the Higgs doublets (H_d, H_u) transform as trivial singlet (1) under A_4. The neutral singlet gauge fermions $S_i(i = 1, 2, 3)$ transform as triplets representation of the A_4 group. In addition to these particles, we have used a flavon ϕ in our work. The purpose of including this flavon is to get a diagonal charged lepton mass matrix without affecting the neutrino sector. Thus this flavon field is considered to be a triplet under A_4. Modular weights is an integral part of modular symmetry. In any model it is very important to assign the appropriate modular weights to its particle content. Accordingly in this work, we have taken the modular weights of lepton doublets to be zero and for the right-handed charged leptons it is -2. Similarly the right-handed neutrinos are assigned modular weights of -2 and rest of the particles (S_i, H_u, H_d) are taken to be of zero modular weights. The flavon is assigned a weight of 2. The charge assignments of the particles under different symmetry groups and their corresponding modular weights have been highlighted in Table (2.1).

	L	E_i	N_1	N_2	S_i	H_u	H_d	ϕ
$SU(2)_L$	2	1	1	1	1	2	2	1
A_4	3	$1, 1'', 1'$	$1'$	$1''$	3	1	1	3
K_I	0	-2	-2	-2	0	0	0	2
Z_3	ω^2	1	ω	ω	1	1	ω	ω

Table 2.1: The above table shows the charge assignments and modular weights of the particles considered in the model. K_I denotes modular weights of the particles.

As mentioned in (1.8.4) of the first chapter, $\Gamma(3)$ modular group has three Yukawa

modular forms of weight two. These Yukawa couplings $Y = (Y_1, Y_2, Y_3)^T$ are functions of the complex modular field τ. Under the symmetry group A_4 these modular forms transform as a triplet. Table (2.2) highlights these informations.

	Y (Modular forms)
A_4	3
K_I	2
Z_3	ω^2

Table 2.2: The charge assignments and weight of Yukawa modular forms for different groups are shown in the above table.

Based on the above discussions on charge assignments, the Lagrangian of the model for the leptonic sector can be written in the following way:

$$-\mathcal{L} = \mathcal{L}_L + \mathcal{L}_D + \mathcal{L}_{NS} + \mathcal{L}_S \tag{2.1}$$

where $\mathcal{L}_L$ is the mass term for charged leptons, $\mathcal{L}_D$ is the Dirac mass term connecting left-handed (ν_L) and right-handed (N_R) components of neutrinos. $\mathcal{L}_{NS}$ represents the mixing term between right-handed neutrinos and sterile fermions (S_i) and $\mathcal{L}_S$ is the Majorana mass term among gauge singlet sterile fermions (S_i). All the terms of the Lagrangian must be invariant under A_4 symmetry group and sum of the modular weights of each term must be zero. Here we denote the vacuum expectation value of H_d and H_u as $\langle H \rangle = v$.

The VEV of the flavon is chosen in the following way [14]:

$$\langle \phi \rangle = (u, 0, 0). \tag{2.2}$$

The Lagrangian for charged leptons take the form:

$$\mathcal{L}_L = \alpha_1 E_1^c H_d (L\phi)_1 + \alpha_2 E_2^c H_d (L\phi)_{1'} + \alpha_3 E_3^c H_d (L\phi)_{1''} \tag{2.3}$$

The parameters $\alpha_1, \alpha_2, \alpha_3$ can be adjusted to get the desired charged lepton masses. With the VEV of the flavon mentioned above, the diagonal mass matrix is obtained as:

$$M_L = diag(\alpha_1, \alpha_2, \alpha_3) uv \tag{2.4}$$

Following the above discussions, the relevant Dirac mass term of the model can be written as follows :

$$\mathcal{L}_D = [N_1(LY)_{1''}H_u]_1 + [N_2(LY)_{1'}H_u]_1 \tag{2.5}$$

where subscripts $(1', 1'', 1)$ represents the irreducible representations of the discrete symmetry group A_4. Subsequently the Dirac mass matrix for the neutrinos is obtained from equation (2.5) in the following form:

$$M_D = v \begin{pmatrix} Y_3 & Y_2 \\ Y_2 & Y_1 \\ Y_1 & Y_3 \end{pmatrix} \tag{2.6}$$

The Majorana mass term for the gauge singlet fermion is:

$$\mathcal{L}_S = \Lambda \ (SS)_1 \tag{2.7}$$

The mass matrix from equation (2.7) can be written as:

$$M_S = \Lambda \begin{pmatrix} 1 & 0 & 0 \\ 0 & 0 & 1 \\ 0 & 1 & 0 \end{pmatrix} \tag{2.8}$$

Similarly, the mixing mass term between the right-handed neutrinos and gauge singlet neutral fermions can be expressed as:

$$\mathcal{L}_{NS} = \beta \ [\{N_1(SY)_{1''}\} + \{N_2(SY)_{1'}\}] \tag{2.9}$$

In equations (2.7) and (2.9) , Λ and β are free parameters. From this Lagrangian mass matrix for the mixing term is obtained as:

$$M_{NS} = \beta \begin{pmatrix} Y_3 & Y_2 & Y_1 \\ Y_2 & Y_1 & Y_3 \end{pmatrix} \tag{2.10}$$

Taking all the mass terms together, we can express the entire Lagrangian in a single 8×8 neutrino mass matrix in the basis $(\nu_i, N_j, S_i)^T$, where $(i = 1, 2, 3)$ and $(j = 1, 2)$. The eigenvalues of this matrix correspond to the mass of the eight fermions, respectively. Finally this single neutrino matrix, in terms of M_D, M_{NS} and M_S can be written as:

$$M_\nu = \begin{pmatrix} 0 & M_D & 0 \\ {M_D}^T & 0 & M_{NS} \\ 0 & {M_{NS}}^T & M_S \end{pmatrix} \tag{2.11}$$

After block diagonalising M_ν, the active light neutrino mass matrix can be written from equation (1.49) in the following way [11, 146, 147]:

$$m_\nu = M_D \,.\, d \,.\, {M_D}^T \tag{2.12}$$

In this way, in the framework of ISS(2,3), we built the first model of this thesis using modular symmetry. Along with A_4 symmetry group, to constrain and restrict certain interaction terms in the Lagrangian, Z_3 is used. Using this model we have calculated the three neutrino mixing angles and its masses. We have also studied the phenomena of neutrinoless double-beta decay and lepton flavor violation in this setup.

2.3 Lepton Number Violation

It has been mentioned that ISS(2,3) contains five extra heavy states which may have significant contributions to lepton number violating processes like neutrinoless double beta decay(NDBD/$0\nu\beta\beta$) [98, 148]. We have studied the effective electron neutrino Majorana mass m_{ee}/m_{eff} [149, 150] characterising $0\nu\beta\beta$ in this model. Experiments like KamLAND-ZEN, GERDA, CUORE and EX0-200 provide stringent bounds on m_{ee}/m_{eff} which can be found in [151, 152, 18].

The decay width of the process is proportional to the effective electron neutrino Majorana mass m_{ee}. In the absence of any sterile neutrino, the standard contribution to m_{ee} can be written as,

$$m_{ee} = \Big| \sum_{i=1}^{3} {U_{ei}}^2 m_i \Big| \tag{2.13}$$

But due to the presence of sterile neutrinos in ISS(2,3), the expression for effective electron neutrino Majorana mass gets modified. As a result, the new expression of m_{ee} after considering the contributions from the heavy fermions can be written as [149]:

$$m_{ee} = \Big| \sum_{i=1}^{3} {U_{ei}}^2 m_i \Big| + \Big| \sum_{j=1}^{5} {U_{ej}}^2 \frac{M_j}{p^2 + M_j^2} | < p > |^2 \Big| \tag{2.14}$$

where U_{ej} represents the coupling of the heavy neutrinos to the electron neutrino and M_j represents the mass of the respective heavy neutrinos. $| < p > |$ is known as neutrino virtuality momentum with value $| < p > | \simeq 190$ MeV.

2.4 Non-Unitarity

In this section, we summarise in short about the non-unitarity of the neutrino mixing matrix. This occurs due to mixing between the light and heavy neutral fermions. In conventional scenerio, this deviation from unitarity can be expressed as

$$U' = (1 - \Theta)\, U_{PMNS} \tag{2.15}$$

where $\Theta \simeq \frac{1}{2}\mathcal{F}\mathcal{F}^{\dagger}$ and $\mathcal{F} \equiv (M_{NS}^{T})^{-1} M_D$ represents the mixing between light and heavy fermions. But due to rectangular shape of M_{NS} and M_D in ISS (2,3), the form of Θ can be written in the following way [153]:

$$\Theta \simeq M_D \left(M_{NS} M_{NS}^{T}\right)^{-1} M_D^{T}/2 \tag{2.16}$$

Several experimental results such as the W boson mass, electroweak universality, CKM unitarity bounds etc. provide constraints on the non-unitarity parameters [154, 155]. In our work, we find that for both the hierarchies, the approximated values of Θ lies in the range $(10^{-6} - 10^{-11})$.

2.5 Lepton Flavor Violation

There are many processes which have been observed in this physical world that have led to pathbreaking scientific discoveries and developments. One of such processes in the field of particle physics are the lepton flavor violating interactions which advocate for a new dimension of physics that surpasses the Standard Model. Through these flavor violating processes, a particular flavor of lepton converts into another flavor. They come in the form of two-body and three-body decay channels. The popular two-body charged lepton flavor violating decay processes are: $\mu \to e\gamma$, $\tau \to e\gamma$, $\tau \to \mu\gamma$. Similarly the three-body decay channels include $\mu \to eee$, $\tau \to eee$ etc. The MEG collaboration experiments, SINDRUM II put bounds on the branching ratios of these decay channels [105, 156].

In ISS(2,3) the 8×8 neutrino mass matrix M_ν can be diagonalised using an unitary matrix to give masses of the eight particles $(m_1, m_2 ....., m_8)$, where the heavy particles are $(m_4, m_5 ..... m_8)$. The mass eigenstates of these eight particles can be represented as N_i, where $(i = 1, 2, ...8)$. The flavor eigenstates of light

active neutrinos (ν_{lL}) can be expressed as a linear combination of these mass eigenstates as:

$$\nu_{lL} = \sum_{i=1}^{8} U_{li} N_i \tag{2.17}$$

The mixing matrix in the above equation is non-unitary. This provides a path to study the charged lepton flavor violating processes in our model.

In this work we have studied the lepton flavor violating decay, $\mu \to e\gamma$. Several experiments with improved sensitivity are searching for this decay mode. Among them the current limit on its branching ratio comes from MEG collaboration, BR($\mu \to e\gamma$)<5.7×10^{-13} [105]. As a result of mixing between active and heavy neutrinos, there is a sizeable contribution to this decay mode in our work. This BR($\mu \to e\gamma$) can be computed in the following way [157, 76]:

$$BR(\mu \to e\gamma) = \frac{\alpha^3 \sin^2\theta_W}{256\pi^2} \left(\frac{m_\mu}{m_W}\right)^4 \frac{m_\mu}{\Gamma_\mu} \quad |G_{\mu e}|^2 \tag{2.18}$$

where m_μ, m_W are masses of μ and W-boson. Γ_μ is the decay width of muon. $G_{\mu e}$ is the loop function given by

$$\begin{aligned} G_{\mu e} &= \sum_i U^*_{\mu i} U_{ei} \;\; G_\gamma\left(\frac{m_i^2}{m_W^2}\right) \\ G_\gamma(x) &= \frac{10 - 43x + 78x^2 - 49x^3 + 4x^4 + 18x^3\log(x)}{3(x-1)^4} \end{aligned} \tag{2.19}$$

With the help of the above relations, we have calculated the BR for the decay $\mu \to e\gamma$. We have presented the results in the following sections of this chapter.

2.6 Numerical Analysis and Results

In this section of the chapter we discuss the processes that we have followed to determine the results of our work. We have discussed them in detail and also have shown the variations among different quantities calculated from the model. For numerical evaluation we have considered the 3σ experimental values of neutrino oscillation parameters [158]. These values have been highlighted in Table (2.3).

Next we diagonalise the light neutrino mass matrix using the relation, $m_\nu = U.\ m_{diag}.\ U^T$, where U is a 3×3 unitary mixing matrix and m_{diag}= diag(m_1, m_2, m_3).

Parameters	Normal Ordering	Inverted Ordering
$\sin^2\theta_{12}$	[0.269,0.343]	[0.269,0.343]
$\sin^2\theta_{23}$	[0.407,0.618]	[0.411.0.621]
$\sin^2\theta_{13}$	[0.02034,0.02430]	[0.02053,0.02436]
$\Delta m^2_{21}/10^{-5}eV^2$	[6.82,8.04]	[6.82,8.04]
$\Delta m^2_{31}/10^{-3}eV^2$	[2.431,2.598]	[2.412,2.583]

Table 2.3: The above table shows the latest 3σ values of neutrino oscillation parameters.

The eigenvalues m_1, m_2, m_3 correspond to mass of the three neutrinos. The mixing angles can be expressed in terms of certain elements of the unitary matrix U. Accordingly, we can write down the relations between the elements of U and mixing angles in the following way [159]:

$$\sin^2\theta_{13} = |U_{e3}|^2, \quad \sin^2\theta_{23} = \frac{|U_{\mu 3}|^2}{1-|U_{e3}|^2}, \quad \sin^2\theta_{12} = \frac{|U_{e2}|^2}{1-|U_{e3}|^2} \tag{2.20}$$

Another important parameter that controls the size of CP violation in quark and lepton sector is the Jarlskog invariant (J_{CP}). It can also be calculated from the elements of the mixing matrix U in the following way:

$$J_{cp} = Im[U_{e1}U_{\mu 2}U^*_{e2}U^*_{\mu 1}] = s_{23}c_{23}s_{12}c_{12}s_{13}c^2_{13}\sin\delta_{cp} \tag{2.21}$$

In order to fit the neutrino oscillation data, we have taken the following range of values for the model parameters:

$$Re(\tau) \to [0,3], \quad Im(\tau) \to [0.5, 2.8], \quad v = 125\ GeV$$

$$\Lambda \to [10,20]KeV, \quad \beta \to [10,100]TeV$$

As the charged lepton mass matrix in this work is diagonal, it has no contribution to the neutrino mixing matrix. Consequently the mixing matrix for neutral sector is governed by the famous $PMNS$ matrix, U_{PMNS}. With the help of this matrix we diagonalise the light neutrino mass matrix for both normal and inverted ordering of neutrino mass spectrum. The solar and atmospheric mass squared differences provide necessary constraints for the model. The values of Λ are taken

in the range (10-20) KeV. Using q-expansions of the modular forms in eq. (1.72), we find out the real and imaginary parts of complex modulus τ, which are found to lie in the range: $\mathrm{Re}(\tau) \to [0, 3]$ and $\mathrm{Im}(\tau) \to [0.5, 2.8]$. The mixing angles from the model can be obtained using the relations given in equation (2.18). The figures representing the corelations among different quantities have been shown in the following sections.

2.6.1 Variation between $\sum m_\nu$ and mixing angles

From cosmological observations it has been found that the latest value for sum of the masses of three neutrinos should be $\sum m_\nu \leq 0.12$ eV. Any model that aims to study neutrino phenomenology must be able to produce this value in the desired range. In figures (2.1) and (2.2), we have shown the variation between sum of neutrino masses ($\sum m_\nu$) and mixing angles $\sin^2\theta_{12}$/ $\sin^2\theta_{23}$ and $\sin^2\theta_{13}$, respectively. From these figures it is evident that for both the mass orderings a large number of values are present within the allowed region as defined by the sum of neutrino masses ($\sum m_\nu < 0.12eV$) and mixing angles. Also it can be seen from Fig.(2.1) that the allowed region of space for atmospheric mixing angle in inverted ordering is much less as compared to normal ordering. This observation indicates that normal ordering is more preferred over the inverted scenario. The lower bound for sum of neutrino masses is found to be around 0.04 eV for both the mass spectrum.

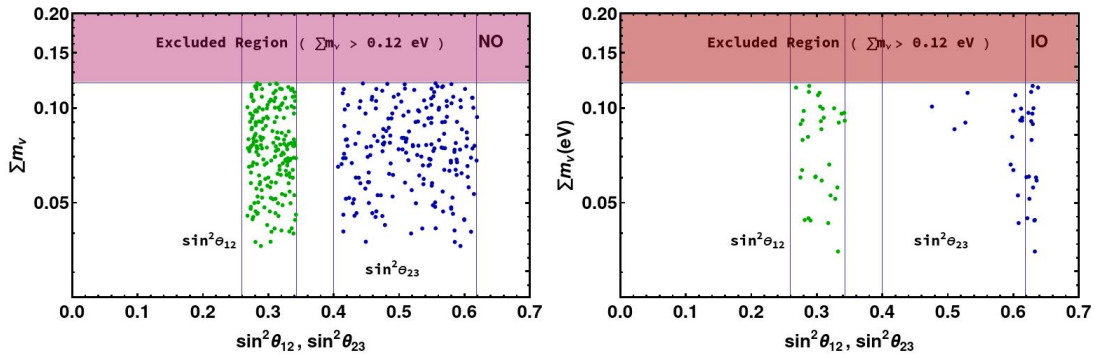

Figure 2.1: The correlation between sum of neutrino masses($\sum m_\nu$) and mixing angles, $\sin^2\theta_{23}$ and $\sin^2\theta_{12}$ for NO (left) and IO(right).

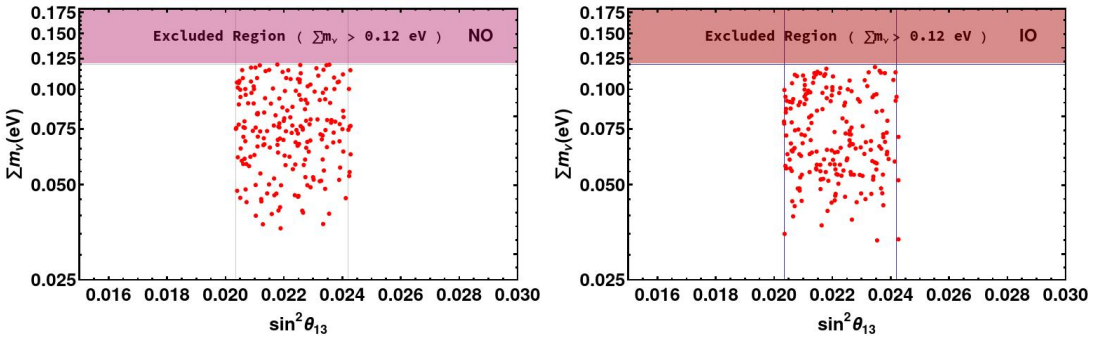

Figure 2.2: The variation of mixing angle, $\sin^2\theta_{13}$ as a function of sum of neutrino masses ($\sum m_\nu$) for NO (left) and IO(right).

2.6.2 Relation among the Yukawa modular forms

In this work we have tried to find favourable regions of the three Yukawa modular forms present in the model. For this purpose, we have studied the variations among Y_1, Y_2 and Y_3 to determine a common region between them. The figures in (2.3) and (2.4) represent this variation between the Yukawa modular forms. It can be seen from Fig. (2.3) that the value of $|Y_1|$ and $|Y_2|$ in case of NO lie within (0.1-1.6) and (0.07-1). While for the IO case, $|Y_1|$ mostly lie in the region (0.5-3) and $|Y_2|$ lie in the region (0.01-1). Similarly from Fig. (2.4), we find that these values for $|Y_3|$ lie within the region (0.009-0.99) and (0.05-1.99) for both normal and inverted ordering, respectively. These values of the yukawa couplings have been summarised below in table (2.4):

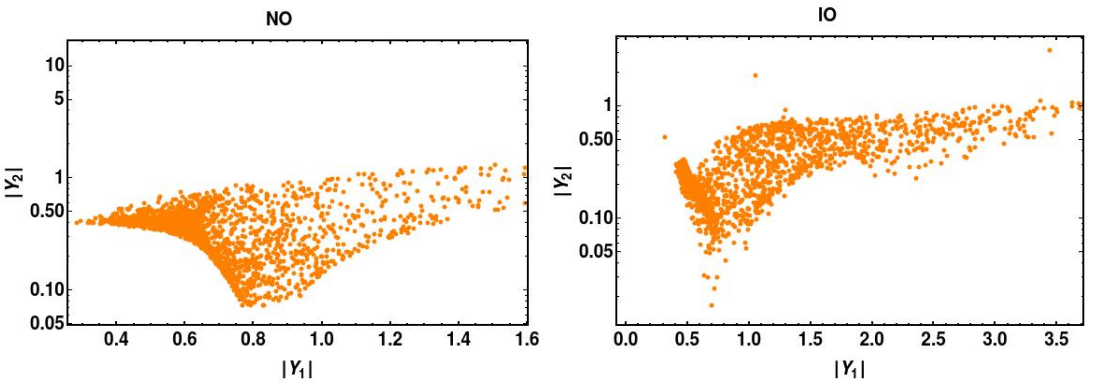

Figure 2.3: Variation between the Yukawa couplings $|Y_1|$ and $|Y_2|$ for both normal and inverted ordering.

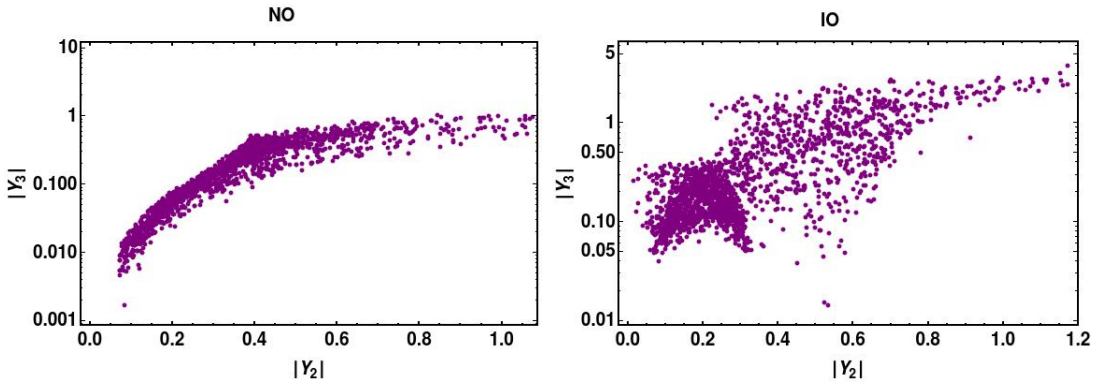

Figure 2.4: The figures show variation between the Yukawa couplings $|Y_2|$ and $|Y_3|$ for both normal and inverted ordering.

	Normal Ordering	Inverted Ordering
$\|Y_1\|$	0.1 - 1.6	0.5 - 3
$\|Y_2\|$	0.07 - 1	0.01 - 1
$\|Y_3\|$	0.009 - 0.99	0.05 - 1.99

Table 2.4: Values (range) of the Yukawa couplings obtained from the model.

2.6.3 Corelation between Yukawa forms and components of τ

In Fig (2.5) we show the variation between Yukawa couplings and real part of the complex modulus, τ for both the mass orderings. It can be observed from the plots that there are certain regions of Re(τ) where the Yukawa couplings are more concentrated. For NO these regions lie near (0.3-0.5) and (2.4-2.8), while for IO it is distributed along the range of Re(τ). The parameter space for the Yukawa coupligs decreases towards right and is mainly confined to the region $<$ 1.5. Similarly, the variations of imaginary part of τ with respect to the Yukawa couplings are shown in Fig. (2.6). Here we find that Yukawa couplings are confined mainly to region (0.8-2.0) of Im(τ) for both the cases. The corelation between Jarlskog invariant and $\sin^2\theta_{23}$ is shown in Fig. (2.7). For both the ordering, there are sufficient values of J_{cp} which lie within the allowed range (-0.04-0.04).

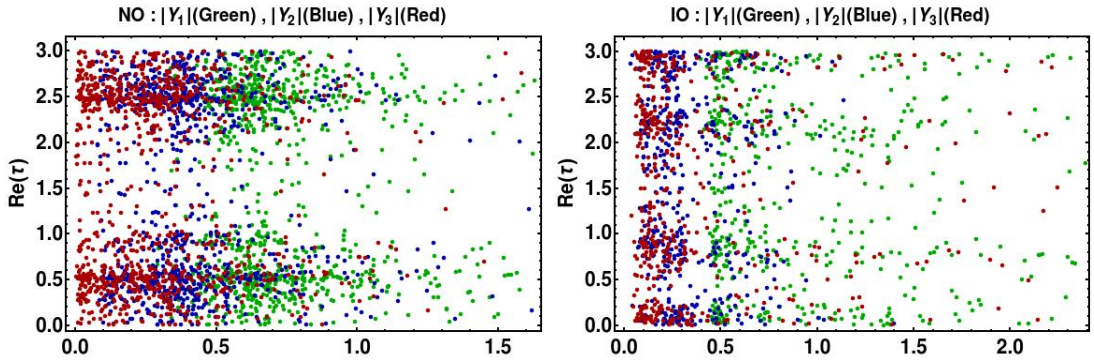

Figure 2.5: Variation of the Yukawa couplings as a function of the real part of τ for NO (left) and for IO(right).

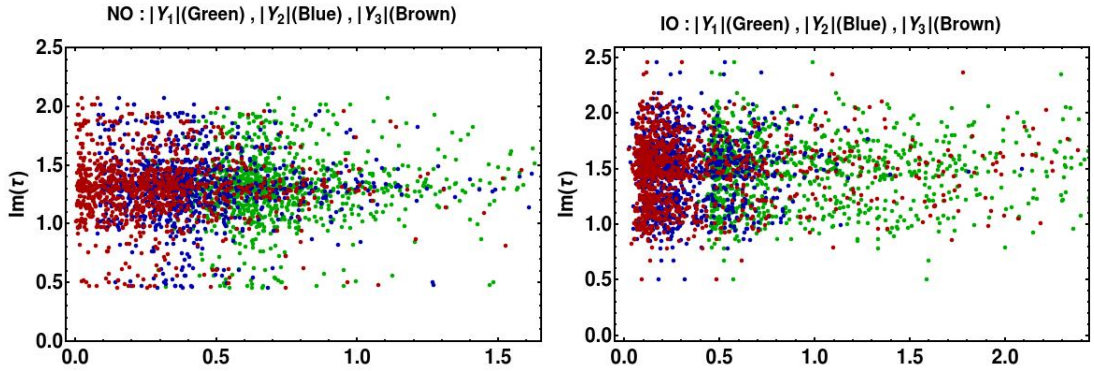

Figure 2.6: Variation of the Yukawa couplings as a function of the imaginary part of τ for NO (left) and for IO(right).

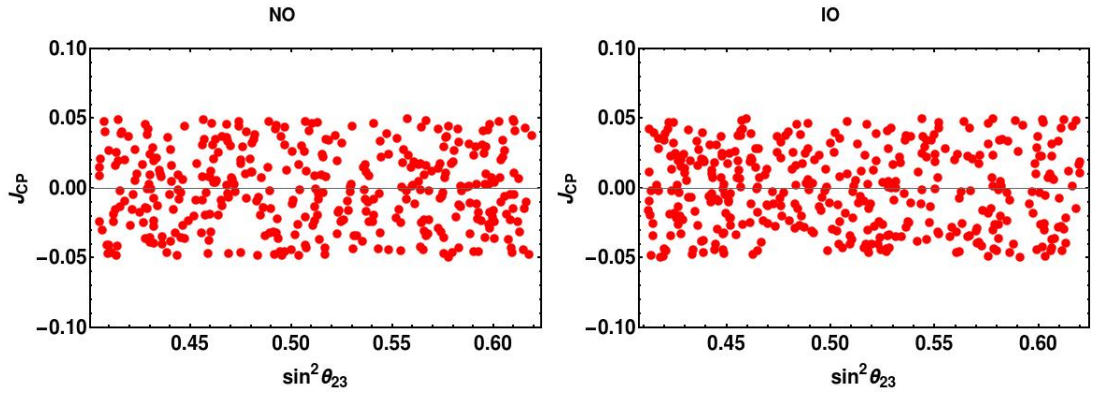

Figure 2.7: Correlation between J_{cp} and $\sin^2\theta_{23}$ for NO (left) and for IO(right).

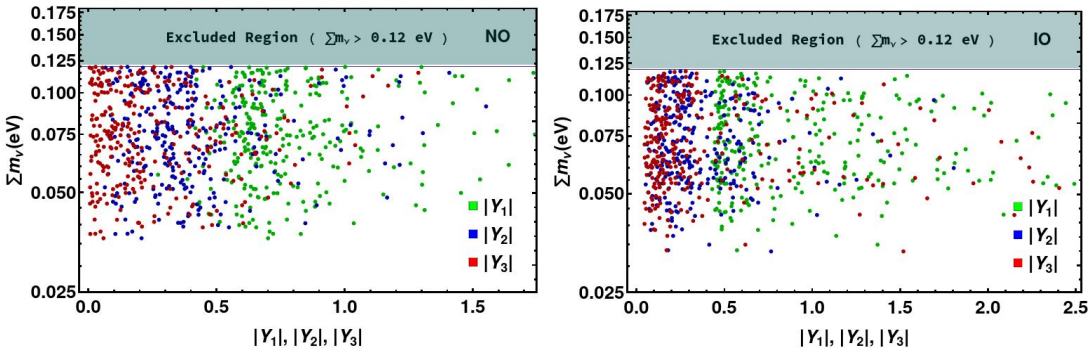

Figure 2.8: Correlation between yukawa couplings ($|Y_1|$ and $|Y_3|$) and $\sum m_\nu$ for NO (left) and for IO(right).

Finally we show the variations between Yukawa couplings, ($|Y_1|$, $|Y_2|$, $|Y_3|$) with sum of neutrino masses ($\sum m_\nu$) in Fig. (2.8). For normal ordering, most of the values of $|Y_1|$ is found to lie in the region (0.5-1) and decreases thereafter. While that of $|Y_2|$ and $|Y_3|$ lie in the regions (0.1-0.4) and (0-0.2). While for inverted ordering, the Yukawa coupling $|Y_1|$ is mostly confined to the region above 0.5 and that of $|Y_2|$ and $|Y_3|$ is mainly spanned in the region (0.1-0.5).

2.6.4 Variation between virtual momentum (p) and m_{ee}

We have calculated the effective electron neutrino Majorana mass (m_{ee}) for both the mass hierarchies. This important parameter is related to neutrinoless double-beta decay which, if detected, has the potential to solve the problem of nature of the neutrinos. In Fig (2.9) we depict the prediction of this model on effective

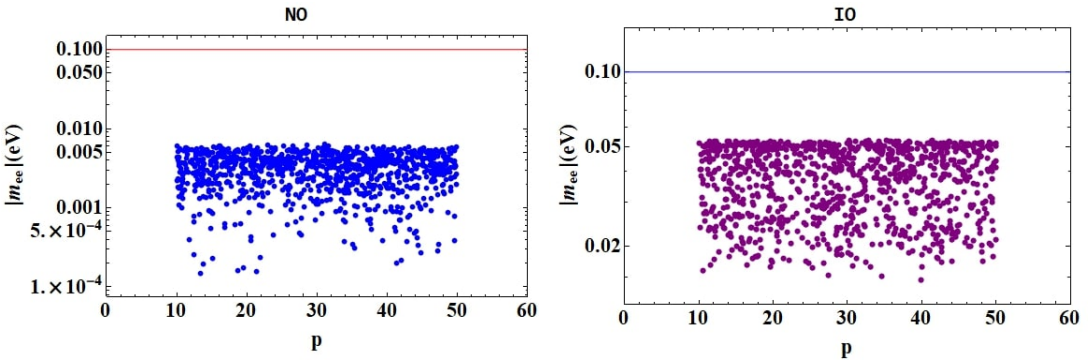

Figure 2.9: Effective mass as a function of parameter p for both normal and inverted hierarchy.

mass characterizing NDBD process for both NO and IO. From these figures we observe that the values of m_{ee} obtained from our work is well below the upper bound of 0.165 eV. For normal ordering the values of m_{ee} are mainly concentrated in the region $(5 \times 10^{-4}$ to 0.008) eV, whereas for inverted ordering it lies around (0.02 to 0.05) eV.

2.6.5 Corelation between BR ($\mu \to e\gamma$) and RHN M_2

Finally we show the results for cLFV process $\mu \to e\gamma$ in the figures (2.10). We have calculated the BR of this process and tried to show its relation with a heavy fermion, M_2. We find that for both the mass hierarchies, a considerable range of its values lie below the current upper bound of BR for $\mu \to e\gamma$ i.e. 5.7×10^{-13}. The parameter space below upper bound for inverted hierarchy is concentrated mainly around BR value of 10^{-16}. So the predicted branching ratio is well below the upper limit.

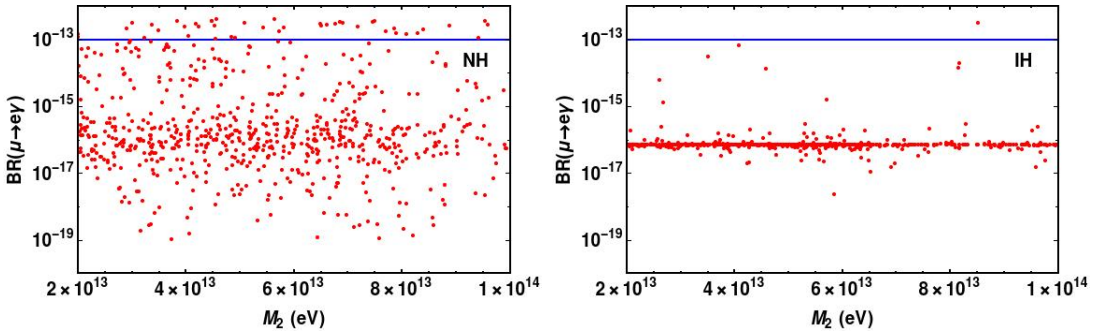

Figure 2.10: The above figures show the corelation between BR ($\mu \to e\gamma$) and M_2 for NH and IH.

2.7 Conclusion

This chapter contains a part of the thesis which includes our work on evaluation of different neutrino parameters i.e mixing angles, sum of neutrino masses and analysis of NDBD and cLFV processes. For this purpose we have constructed a model in the framework of minimal inverse seesaw, ISS(2,3). As we have used A_4 modular symmetry in this model, the number of flavons is significantly reduced and we needed only one flavon in this work. This is a major adavantage of using

modular symmetry in model building. In addition to A_4 group, we have also used the abelian discrete symmetry group Z_3 which acts as filter to remove certain unwanted interactions of the models. We have studied the neutrino parameters for both normal as well as inverted hierarchy. A reasonable range of the sum of active neutrino mass ($\sum m_\nu$) is found to lie within the upper bound i.e. 0.12 eV. Also a possible lower value is found to lie around 0.03 eV. The predicted allowed parameter space consistent with the experimental value of atmospheric mixing angle is found to be larger in normal hierarchy than the one corresponding to inverted hierarchy. The Yukawa couplings are constrained and found to lie mostly in the region (0.08-0.5). Also we have studied NDBD and cLFV for both the hierarchies. Accordingly we have calculated the effective mass of electron neutrino for both the mass hierarchies. Similarly we have found out the branching ratio for the cLFV process $\mu \to e\gamma$ in this model. We find that the values of these parameters lie within the allowed range as predicted by different experiments, thereby, justifying the validity of this model.